Aggregated Model of a Distributed PV Plant Using the Synchronous Power Controller

Daniel Remon*‡, Antoni M. Cantarellas*‡, Juan Diego Nieto*‡, Weiyi Zhang‡, Pedro Rodriguez*‡

*Abengoa Research, Abengoa
Campus Palmas Altas, Seville, Spain 41014
Email: daniel.remon@abengoa.com
‡Department of Electrical Engineering
Technical University of Catalonia
GAIA Building, Terrassa, Barcelona, Spain 08222

Abstract—**Power plants employing renewable energy sources connected to large power systems continue increasing their number and size. PV and wind farms are a clear example of this trend. They employ power electronics in order to inject power in the grid and in most cases the interaction does not take into account the power system needs. However, as their size increases, these plants should support the grid with ancillary services and it is necessary to analyze their impact on the grid.**

Despite large conventional power plants usually comprise a small amount of synchronous generators in the range of 100 MW, large power plants using power electronics are formed by a relevant number of individual generating units in the 1 MW range, which introduces additional complexity in the analysis of power systems. Therefore, it is necessary to develop aggregated models of distributed power plants. This paper presents the control of a 20 MW PV power plant and an equivalent model, which is validated through simulation.

Index Terms—**grid support, power plant equivalent, power system stability, renewable energy sources.**

I. INTRODUCTION

The increase of the penetration of renewable energy sources is expected to be maintained during the next years owing to environmental policies and the cost reduction of the technology [1]. Apart from residential, industrial or campus installations, these sources also power large generating stations, able to reach ratings over $100 \, \text{MW}$. This is the case of concentrated solar power plants using synchronous generator, but also of PV and wind power plants, which are connected to the grid through power electronics converters.

Power generating stations connected to the power system through power electronics do not usually behave like synchronous generators, the backbone of classical electrical systems [2]. Therefore, taking into account plants in the range of $100 \, \text{MW}$, it is necessary to analyze the impact that plants using power electronics have on the grid, and to propose control concepts that allow these plants to interact with it harmoniously, contributing to its control and stability as required by system operators.

Power system operators require nowadays that new plants based on power electronics provide frequency and voltage regulation [3], and are also interested in services like power oscillation damping and inertia emulation. This is particularly necessary when conventional power plants using synchronous machines that provide ancillary services are replaced by power electronics. Taking this into account, several authors have proposed embedding the behavior of synchronous machines to some extent in converter control systems [4]–[7]. The synchronous power controller (SPC) presented in [7] is a flexible solution that considers the swing equation of a synchronous machine and improves its response with additional damping and adaptability to different frequencies.

When it comes to the analysis of power systems considering these plants, it is necessary to take into account that it usually involves a large number of generating units with power ratings in the range of $100 \, \text{MW}$, whereas large power plants based on power electronics are normally formed by a large amount of small units, whose power rating is around $1 \, \text{MW}$. In this case, a detailed model can provide useful information in a dynamic analysis, but it can also lead to long simulation times and even to numerical errors because of the different power ranges involved. Therefore, it is convenient to obtain equivalent models of distributed power plants, aggregating units and thus reducing the number of variables and equations in the analysis.

In this paper, an aggregated model of a PV power plant is presented. The power plant is formed by 20 SPC-based converters whose power rating is $1 \, \text{MW}$.

II. POWER PLANT STRUCTURE AND CONTROL

A. Power Plant Structure

This paper studies a power plant connected to a $50 \, \text{Hz}$, $33 \, \text{kV}$ grid. The plant is composed of 20 PV generating units equally distributed over two identical feeders and its single line diagram is shown in Fig. 1. Each feeder connects five buses to the point of common coupling of the plant, with two generating stations connected through independent $33/0.365 \, \text{kV}$ transformers to each bus.

The section and length of the cables is designed taking into account the plant layout and their power transfer requirements
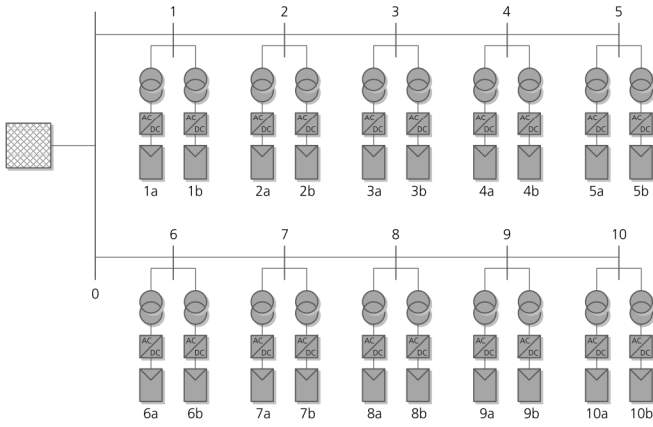
Fig. 1. Single-line diagram of the power plant.

TABLE I
CHARACTERISTICS OF CABLES

Cable	L (m)	R (Ω)	X (Ω)	C (uF)	I_r (kA)
0-1, 0-6	600	0.04590	0.07518	0.1158	0.440
1-2, 6-7	250	0.01913	0.03133	0.04825	0.440
2-3, 7-8	250	0.03118	0.03385	0.04150	0.350
3-4, 8-9	250	0.03118	0.03385	0.04150	0.350
4-5, 9-10	250	0.04823	0.03620	0.03650	0.281

and their main characteristics are summarized in Table I. The transformers, with a rated power of $1.15\,\text{MVA}$, have a short circuit voltage $\varepsilon_{cc} = 9\%$ and copper losses of $3.45\,\text{kW}$.

The stations are formed by a voltage source converter whose rated AC voltage and power are respectively $365\,\text{V}$ and $1.25\,\text{MVA}$, designed to operate at a 0.8 power factor, and the associated PV array with a peak power of $1.2\,\text{MW}$. The converters are connected to the grid through an LCL filter that mitigates the harmonic injection.

B. Power Plant Control

The stations in the power plant share the plant active and reactive power references through constant participation factors that can be updated periodically in order to adapt to the availability of the resource and the scheduled power plant production and voltage profile.

The dynamic response of the plant, including its contribution to frequency and voltage regulation, is the result of the independent response of all the stations, which employ local measurements. Due to the speed of power converters, their response depends on its control loops, which are explained below.

1) Inner controllers: The converters use a pulse width modulation that determines the state of the power switches. The modulation follows a converter voltage reference generated by a current controller, whose commitment is to track a current reference provided by the outer controller. The converter, the modulation and the current loop have a fast response and it is possible to model the converter with its inner loops as a controlled current source that injects the current reference with
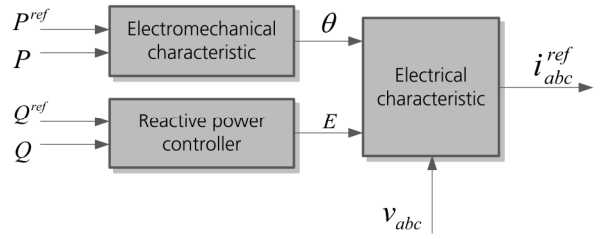

Fig. 2. Constituting blocks of the synchronous power controller.

a delay represented by a first-order low-pass filter with a time constant $\tau = 5\,\text{ms}$.

2) The synchronous power controller: The current reference is given by the synchronous power controller. The SPC reproduces a simplified electrical model and the swing equation of a synchronous machine and is composed of three blocks, as depicted in Fig. 2.

The electrical characteristic of the SPC reproduces an electromotive force behind an impedance. It takes the internal voltage magnitude generated by the reactive power controller and the angle provided by the electromechanical characteristic block and calculates the corresponding three-phase instantaneous voltage. This voltage is compared with the measurement after the grid-connection filter, and their difference determines the voltage drop through the virtual impedance, which induces a current given by (1). In small signal, the transfer function between the voltage drop and the current is (2).

$$\frac{di}{dt} = \frac{1}{L}\left(\Delta v - Ri\right) \tag{1}$$

$$\frac{\Delta i}{\Delta v}(s) = \frac{1}{R + Ls} \tag{2}$$

The electromechanical characteristic of the SPC is based on the swing equation of a rotating mass with a damping term, like in (3), where ω is the rotor speed, J is its moment of inertia, D is the damping coefficient and P_{mech} and P_{elec} are respectively the input and output power. The flexibility of a converter allows modifying the moment of inertia and the damping coefficient in real time in order to adapt them to the state of the grid. Exploiting that, the SPC employs a small signal version of (3), given by (4), and it results in the active power loop shown in Fig. 3, with the desired moment of inertia and damping coefficient because its closed-loop transfer function is (5).

$$J\frac{d\omega}{dt} = \frac{P_{mech} - P_{elec}}{\omega} - D\Delta\omega \tag{3}$$

$$\frac{\Delta\omega}{\Delta P}(s) = \frac{1}{J\omega}\frac{1}{s + 2\zeta\sqrt{\frac{T_P}{J\omega}}} \tag{4}$$

$$\frac{\Delta P_{out}}{\Delta P_{ref}}(s) = \frac{\frac{T_P}{J\omega}}{s^2 + 2\zeta\sqrt{\frac{T_P}{J\omega}}s + \frac{T_P}{J\omega}} \tag{5}$$
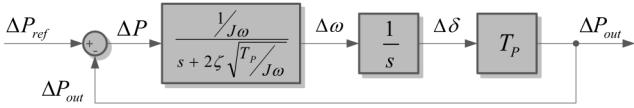
Fig. 3. Active power loop with the synchronous power controller emulating inertia J with damping coefficient ζ.

Cable	R (pu)	X (pu)
0-1, 0-6	$8.430 \cdot 10^{-4}$	$1.381 \cdot 10^{-3}$
1-2, 6-7	$3.512 \cdot 10^{-4}$	$5.753 \cdot 10^{-4}$
2-3, 7-8	$5.725 \cdot 10^{-4}$	$6.217 \cdot 10^{-4}$
3-4, 8-9	$5.725 \cdot 10^{-4}$	$6.217 \cdot 10^{-4}$
4-5, 9-10	$8.857 \cdot 10^{-4}$	$6.648 \cdot 10^{-4}$

The reactive power controller is a proportional, integral controller that cancels the reactive power error by actuating on the internal voltage magnitued E.

3) Higher-level controllers: In addition to these loops, the SPC active and reactive power references are modified in order to contribute to frequency and voltage regulation. This is achieved by two equivalent droop blocks. The frequency droop uses the internal SPC frequency estimation to modify the active power reference, whereas the voltage droop takes the measurement of the voltage after the converter grid-connection filter and determines the resulting reactive power reference.

III. POWER PLANT EQUIVALENT MODEL

In order to develop the equivalent model, the power plant is first represented in per unit, taking a base voltage of $33\,\text{kV}$ and a base power of $20\,\text{MVA}$.

The per unit values of the impedances associated to the cables are given in Table II, the transformer per unit impedance is $\underline{Z}_{tr} = 0.05217 + 1.565j$, and the virtual impedance and internal voltage of the converters have to be considered as variables.

The equivalent model aims to represent the plant as an SPC converter with its internal voltage and virtual impedance behind an equivalent impedance representing the cables and transformers.

Taking into account the data in Table II and the transformer impedance, the impedance of the cables can be neglected in the aggregated model in front of the impedance of the transformers. Therefore, a model analogous to Fig. 4 can be considered, together with its Thévenin equivalent, which is given by (6).

$$\underline{U}_{th} = \frac{\sum_{k=1}^{n} \dfrac{\underline{U}_k}{\underline{Z}_k}}{\sum_{k=1}^{n} \dfrac{1}{\underline{Z}_k}} \qquad \underline{Z}_{th} = \frac{1}{\sum_{k=1}^{n} \dfrac{1}{\underline{Z}_k}} \tag{6}$$
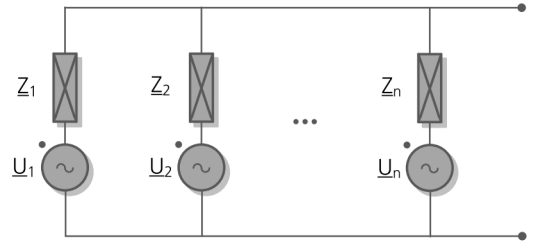

Fig. 4. Single-line diagram of a system formed by an arbitrary number of voltage sources connected to a common bus.

Applying (6) with $\underline{U}_k$ equal to the converter terminal voltages and $\underline{Z}_k = \underline{Z}_{tr}$, the impedance representing the transformers is obtained as their parallel equivalent, it is possible to obtain the equivalent impedance representing the transformers, which is given by $\underline{Z}_t = \frac{\underline{Z}_{tr}}{20} = 0.002609 + 0.07826j$. The plant can be thus represented by a new simplified model consisting of the equivalent transformer impedance Z_t, a common bus and the SPC converters with their virtual impedance and internal voltage.

On the other hand, if all the converters have equal parameters and are working in the same conditions, their internal voltage will be the same, so they can be represented by a single voltage source to which all virtual impedances are connected. Finally, these virtual impedances can be aggregated as their parallel equivalent.

Additionally, the equivalent model of the virtual internal voltage source requires defining the corresponding electromechanical parameters. The inertia of the equivalent machine must represent the total inertia of the plant. Therefore, its per unit inertia H is given by (7), where $H_{i\alpha}$ and $S_{b,i\alpha}$ are the per unit inertia and the base power for each converter and $S_{b,plant} = 20\,\text{MVA}$ is the base power of the plant. Since all converters share a common base power $S_{b,i\alpha} = 1\,\text{MVA}$, H is the average value of all $H_{i\alpha}$. When all the converters emulate the same moment of inertia, this average value coincides with the per unit value of each machine.

$$H = \frac{\sum_{i=1}^{10} \left(H_{ia} S_{b,ia} + H_{ib} S_{b,ib} \right)}{S_{b,plant}} \tag{7}$$

Similarly, the reactive power controller gains and the droop coefficients of the aggregated model have the same per unit values as a single machine if all the converters share a common set of parameters.

IV. RESULTS

The equivalent model is validated with the detailed model of the plant. In this section, the response to the plant to different disturbances is studied with both models using DIgSILENT PowerFactory. In the simulations, all the converters in the power plant share the same parameters and initial references, given in Table III in the station per unit system, with a base power of $1\,\text{MVA}$. The aggregated model has the same per unit

TABLE III
STATION PARAMETERS AND POWER REFERENCES

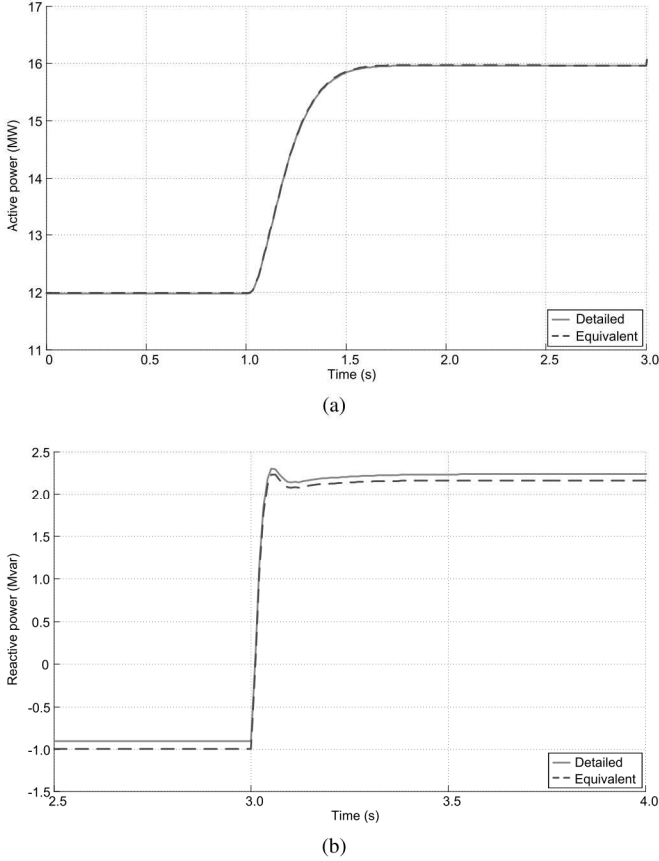| Magnitude	Value	Unit
Base power	1	MVA
Virtual resistance	0.05	pu
Virtual reactance	0.30	pu
Moment of inertia	5	s
Damping coefficient	0.8	pu
Frequency droop coefficient	0.05	pu
Voltage droop coefficient	0.05	pu
Active power reference	0.6	pu
Reactive power reference	0.0	pu

(a)

(b)

Fig. 5. Power injections of the detailed model (solid line) and the equivalent model (dashed line) of the plant: (a) Active power response to a step at $t = 1\,\text{s}$. (b) Reactive power response to a step at $t = 3\,\text{s}$.

parameters for a base power of $20\,\text{MVA}$. On the other hand, the grid is modeled by its Thévenin equivalent, constituted by a real $50\,\text{Hz}$, $33\,\text{kV}$ voltage source with a short-circuit current of $10\,\text{kA}$ and a resistance-to-reactance ratio equal to 0.1.

A. Reference Step

The first test case evaluates the response of the plant to changes in its active and reactive power references. In order to do that, the active power reference is increased to $0.8\,\text{pu}$ at $t = 1\,\text{s}$ and the reactive power reference changes from $0\,\text{pu}$ to $0.45\,\text{pu}$ at $t = 3\,\text{s}$ and the results are shown in 5.
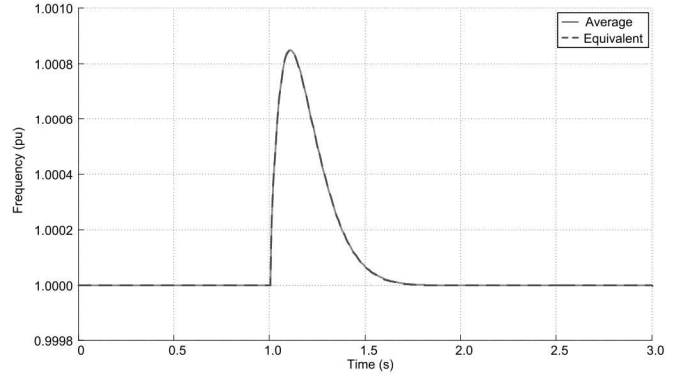

Fig. 6. Average frequency response in the detailed model (solid line) compared to the frequency response in the equivalent model (dashed line).
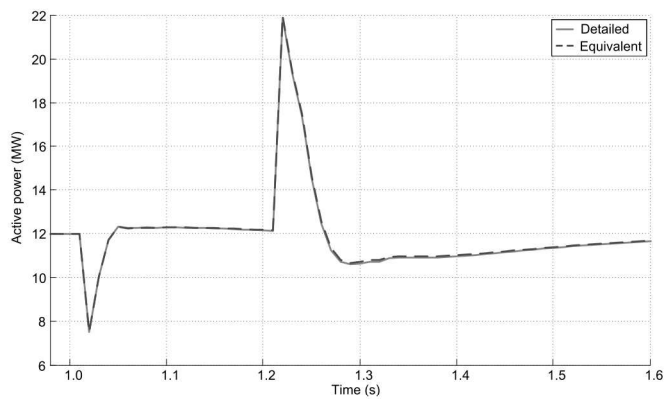
Fig. 5a shows the active power response, which has the dynamics of a first-order system. The active power injected by the equivalent model of the plant reproduces the dynamics of the P injection in the detailed model without observable differences during the transient. In fact, these differences are below 0.1% of the rated power of the plant during the whole simulation. On the other hand, Fig. 5b is a plot of the reactive power response of both models, where it is possible to see that the injected reactive power does not reach its reference in any case because of the droop response of the plant and the voltage rise due to the injection of active power. With the reactive power it is possible to see a small steady-state difference between both models. However, the maximum error is around 0.5% of the rated power of the plant. Therefore, the errors introduced by the equivalent model can be considered acceptable.

Furthermore, the analysis can include the evolution of the frequency during the active power step in both models. Since the frequency of all the converters is very similar in the detailed model, with slight differences among converters depending on the impedance between them and the point of common coupling, an average value is used in order to obtain a clearer plot. This average value is compared with the frequency estimated by the aggregated SPC in Fig. 6. As in the case of active power, this figure shows how accurate the equivalent model is, reproducing almost exactly the average frequency in the plant.
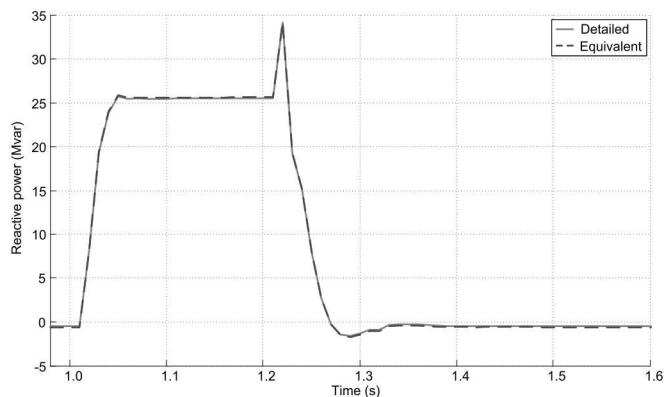
B. Grid Voltage Sag

The second test case considers a sudden reduction in the RMS value of the grid voltage. The voltage of the source representing the grid is reduced to $0.5\,\text{pu}$ at $t = 1\,\text{s}$ and recovers its initial value at $t = 1.2\,\text{s}$.

The results in the power injections are shown in Fig. 7. The evolution of the active power is given in Fig. 7a. At the beginning of the sag, the active power injected by the plant decreases because of the reduction of the grid voltage. However, the voltage and reactive power controller react quickly and allow the plant to recover its initial capacity to inject power into the grid, so that it recovers its initial injection

(a)

(b)

Fig. 7. Power injections of the detailed model (solid line) and the equivalent model (dashed line) of the plant: (a) Active power response to a voltage sag. (b) Reactive power response to a voltage sag.
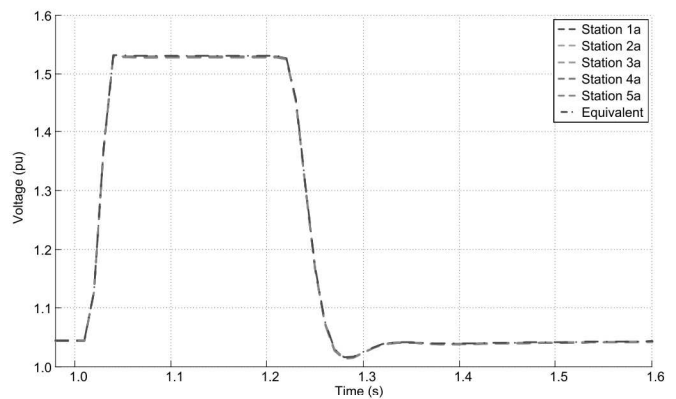

Fig. 8. Internal voltage magnitude of representative stations compared to the plant internal voltage magnitude in the equivalent model during a voltage sag.

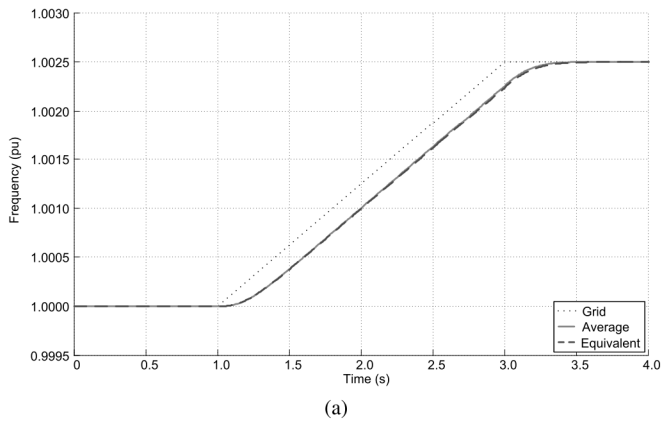among them – are considered.

C. Grid Frequency Ramp

Finally, the response of the plant to a grid frequency imbalance is tested. The frequency imbalance considered here is a ramp increase, which can be due to the temporal disconnection of a large load due to a fault. The ramp starts at $t = 1\,\text{s}$ and lasts for $2\,\text{s}$. From $t = 3\,\text{s}$ on, the frequency is stabilized at its final value, which is $1.0025\,\text{pu}$.

Fig. 9 shows the evolution of the frequency in the grid and the plant response. Fig. 9a is a plot of the evolution of the grid frequency, the average frequency of the SPC converters in the detailed model and the frequency of the equivalent model, which reproduces the results of the detailed model with great accuracy. It can be observed that the plant follows the variations in the grid with a short delay, caused by the emulated inertia, and reaches a final steady state in synchronism with the power system.
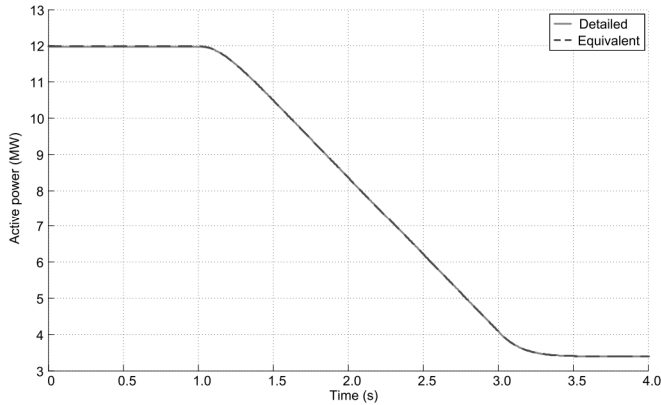
The active power response of the plant to this event can be seen in Fig. 9b. Here it can be observed how the plant reacts to the frequency rise, decreasing its active power injection. This decrease is caused by the plant droop, but also by the active power loop itself, which introduces an additional steady-state droop because of the damping term. As in the previous tests, the results of the aggregated model reproduce those obtained with the detailed one.

V. CONCLUSION

This article presents a PV power plant formed by 20 power conversion stations of $1\,\text{MW}$, whose interaction with the power system is determined by the synchronous power controller. This controller allows converters to interact synchronously with the power system and makes them able to provide the same services as conventional generators while avoiding some drawbacks, like their slight damping. Considering the topology of the plant and its control structure, an equivalent model of the plant is derived. This model aggregates all the power converters in the plant into a single one, which is also controlled by the synchronous power controller.

level in $50\,\text{ms}$. Afterwards, when the grid voltage is restored to its rated value, the active power injection suddenly surges, due to the high values of current necessary to maintain the power injection during the sag. The controllers adapt again the power injection so that it takes back its reference value.

The evolution of reactive power is plotted in Fig. 7b. Due to the effect of the voltage droop and the reactive power controllers, the plant reacts with a fast increase and a fast decrease in the reactive power injection in front of the voltage fall and rise respectively. During the sag, the total apparent power generated by the plant is over $25\,\text{MVA}$, so it is overloaded. Nevertheless, this overload is soon cleared, so the devices may be able to withstand it without suffering a failure.

The variations in the reactive power injection are achieved through the modification of the internal voltage magnitude, as shown in Fig. 8. In fact, this plot allows seeing how the internal voltage magnitude reaches its upper bound, $1.53\,\text{pu}$, and saturates the integrator. After the sag, the reactive power controller sets the internal voltage magnitude back to its previous value.

In Fig. 7 and 8, the equivalent model reproduces the results of the detailed model with great accuracy, both in the case of the total active and reactive power injection and when the individual internal voltages of the stations – very similar

(a)

(b)

Fig. 9. Response of the plant to a grid frequency ramp in the detailed model (solid line) and the equivalent model (dashed line): (a) Frequency measurement. (b) Active power response.

The equivalent model is compared with the complete model through simulation in front of different disturbances, such as reference modifications, a grid voltage sag or a frequency ramp. The results provided by the equivalent model reproduce with great accuracy those obtained with the complete one, which makes the equivalent model highly useful and valuable, since it can be successfully applied to the analysis of large power plants without losing precision or increasing the complexity of the whole power system model excessively.

REFERENCES

[1] International Energy Agency, *World Energy Outlook 2014*. Paris: OECD/IEA, 2014.

[2] P. Kundur, *Power System Stability and Control*. New York: McGraw-Hill, 1994.

[3] *ENTSO-E Network Code for Requirements for Grid Connection Applicable to all Generators*, ENTSO-E Std., Mar 2013.

[4] H. Bevrani, T. Ise, and Y. Miura, "Virtual synchronous generators: A survey and new perspectives," *Electrical Power and Energy Systems*, vol. 54, pp. 244–254, 2014.

[5] L. Zhang, L. Harnefors, and H.-P. Nee, "Power-synchronization control of grid-connected voltage-source converters," *Power Systems, IEEE Transactions on*, vol. 25, no. 2, pp. 809–820, May 2010.

[6] C.-H. Zhang, Q.-C. Zhong, J.-S. Meng, X. Chen, Q. Huang, S.-H. Chen, and Z. peng Lv, "An improved synchronverter model and its dynamic behaviour comparison with synchronous generator," in *Renewable Power Generation Conference (RPG 2013), 2nd IET*, Sept 2013, pp. 1–4.

[7] P. Rodriguez, I. Candela, and A. Luna, "Control of PV generation systems using the synchronous power controller," in *Energy Conversion Congress and Exposition (ECCE), 2013 IEEE*, Sept 2013, pp. 993–998.